Andean Geology 45 (3): 357-378. September, 2018 doi: 10.5027/andgeoV45n3-2974

Factors controlling alpine glaciations in the Sierra Baguales Mountain Range of southern Patagonia (50° S), inferred from the morphometric analysis of glacial cirques

*José M. Araos^{1, 2}, Jacobus P. Le Roux^{1, 3}, Michael R. Kaplan⁴, Matteo Spagnolo⁵

- ¹ Programa de Doctorado en Ciencias, mención Geología, Departamento de Geología, Facultad de Ciencias Físicas y Matemáticas, Universidad de Chile, Plaza Ercilla 803, Santiago, Chile. josearaos@ug.uchile.cl
- ² Departamento de Geografia, Universidad Alberto Hurtado, Cienfuegos #41, Santiago, Chile. jaraos@uahurtado.cl
- ³ Andean Geothermal Centre of Excellence, Universidad de Chile, Plaza Ercilla #803, Santiago, Chile. jroux@ing.uchile.cl
- ⁴ Lamont-Doherty Earth Observatory of Columbia University, Palisades, 61 Route 9W, Palisades, NY 10964-1000 USA mkaplan@ldeo.columbia.edu
- ⁵ School of Geosciences, University of Aberdeen, Aberdeen, UK AB243UF. m.spagnolo@abdn.ac.uk
- $*\ Corresponding\ author: joseara os@ug.uchile.cl$

ABSTRACT. The Sierra Baguales Mountain Range, forming the eastern foothills of the Southern Patagonian Andes, has well-developed alpine-glaciated landforms which present an ideal opportunity to study climatic and non-climatic factors that control cirque development and morphology. One hundred and forty-three glacial cirques were studied with reference to 14 morphometric attributes which were analyzed using statistical analysis and GIS methodologies. The cirques were classified into two types using cluster analysis complimented with a composite map based on the attributes, the latter technique that is applied to glacial cirque analysis for the first time. Type 1 cirques are associated with glacial processes isolated from the Southern Patagonian Ice Field (SPIF), developed under locally cold and dry climatic conditions. Type 2 glacial cirques are associated with older, more extensive glacial processes controlled by regional-scale climate variables and the presence of the Pleistocene Ice Sheet. The results show that the development of most of the glacial cirques has been controlled mainly by their aspect, exposure to solar radiation, Southern Hemisphere Westerly winds, and cirque floor slope. Finally, we concluded that our analyses show the evolution of cirques in the Sierra Baguales Mountain Range was not uniform. Cirque glaciers that developed to the west, close to the Southern Patagonian Ice field, have been more dynamic, and therefore their cirques experienced more erosion than those located to the east.

Keywords: Cirque, Sierra Baguales Mountain Range, Glacial geomorphology, Alpine glaciation, Southern Patagonia.

RESUMEN. Factores de control sobre las glaciaciones alpinas del cordón montañoso de Sierra Baguales (50° S), inferidos del análisis morfométrico de circos glaciales. El cordón montañoso de Sierra Baguales, estribación oriental de Los Andes Patagónicos, muestra evidencia del desarrollo de circos glaciales de tipo alpino, morfologías características del relieve de montaña, cuyo desarrollo puede ser controlado por variables climáticas y no climáticas. El área de estudio representa por tanto, un sitio ideal para estimar aquellos factores que controlaron el desarrollo de glaciaciones confinadas a circos glaciales. Ciento cuarenta y tres de estos circos fueron estudiados considerando 14 atributos morfométricos,

los que fueron analizados mediante el uso de Sistemas de Información Geográfica (SIG) y metodologías estadísticas. Un análisis estadístico de tipo "cluster", complementado con el desarrollo de un mapa compuesto, técnica aplicada por primera vez en el análisis de circos glaciales, permitió diferenciar dos tipos ellos: El Tipo 1 representa circos aislados de la influencia del Campo de Hielo Sur, desarrollados bajo condiciones climáticas frías y secas, de carácter local. El Tipo 2 representa circos asociados a glaciaciones más extensas y antiguas, donde los glaciares evolucionaron bajo condiciones climáticas de escala regional y la influencia del Campo de Hielo Sur. Los resultados muestran que la evolución de los circos glaciares del tipo alpino fue controlada por factores tales como la exposición de los glaciares a la radiación solar y a los vientos del oeste (Westerlies), además de la pendiente del piso de los circos glaciales. El desarrollo de estos circos glaciales no fue uniforme, puesto que los glaciares alpinos más cercanos al Campo de Hielo Sur fueron más masivos y dinámicos en comparación con aquellos ubicados hacia el oriente de la estribación andina.

Palabras clave: Circo glaciar, Cordón montañoso de Sierra Baguales, Geomorfología glacial, Glaciación alpina, Patagonia austral.

1. Introduction

The Cenozoic history of the southern Andes has been largely influenced by the relationship between tectonic uplift, climate, and glaciations (Montgomery et al., 2001; Ramos and Ghiglione, 2008; Kaplan et al., 2009). The region contains ample geomorphological evidence of continental glaciations of different ages and extents (Rabassa and Coronato, 2009; Rabassa et al., 2011). This is especially true for the outlet glaciers of the Southern Patagonian Ice Field (SPIF), the dynamics of which were related to climate, in particular the latitudinal displacement and changes in the intensity of the Westerly winds (Hulton et al., 1994; McCulloch et al., 2000; Hulton et al., 2002; Rabassa et al., 2005; Sugden et al., 2005; Rodbell et al., 2009). However, far less attention has been paid to the characteristics and behavior of former alpine glaciations in southern South America, specifically individual and small, independent cirque glaciers that have developed, evolved, and in many cases disappeared in the proximity of the SPIF.

The study of alpine-glaciated landscapes in Patagonia is important because it provides a sensitive proxy for paleoclimate settings. Geomorphological evidence is useful to highlight the factors that controlled the development of cirque-type glaciation, such as the regional snow-line, dominant wind direction, rain shadow, and insolation effects (e.g., Evans, 1977; Olyphant, 1981; Federici and Spagnolo, 2004; Evans, 2006; Hughes et al., 2007; Křížek et al., 2012; Delmas et al., 2013; Barr and Spagnolo, 2015). In this study, we examine glacial cirque features in the Sierra Baguales Mountain Range (SBMR), a large glaciated range beyond the main cordillera spine, topographically isolated from the SPIF, and influenced by the Westerlies winds and associated climates (Villa-Martínez and Moreno, 2007). Cirques are one typical and frequent SBMR glacial landforms, many of which are still occupied by small glaciers or permanent snow patches.

The aims of this study are to describe and analyze glacial cirques located around 50° S, in an area which had not been investigated before, and to evaluate the possible controlling factors in their development. Our description of the morphometric characteristics of glacial cirques is based on the interpretation of aerial photos, satellite images and field mapping. Data analysis was conducted using GIS and statistical software.

2. Study area

2.1. Climatic and geological setting

The Andean Patagonian Massif was formed during the Andean Tectonic Cycle (late Early Jurassic-present), and is a product of subduction accompanied by a succession of extensional and contractional episodes related to changes in the dynamics, geometry and convergence speed of the Farallon and South American Plates (Charrier *et al.*, 2007). The Andean Patagonian Massif forms a magmatic arc that corresponds to the western boundary of the Magallanes Basin (Ramos, 1989; Diraison *et al.*, 2000).

Relative recent uplift of the Patagonian Andes resulted mainly from a strong increase in the convergence rate and a decrease in the obliquity between the plates (Charrier *et al.*, 2007; Ramos and Ghiglione, 2008). At about 14 Ma, the southern Andes focused on here, reached its maximum elevation and the rain shadow effect intensified, continuing throughout the Quaternary. According to Ramos and Ghiglione (2008), the orographic effect of the Andes generated a climatic contrast

in southern Patagonia and influenced the styles of development of continental and alpine glaciations during the Last Glacial Maximum (LGM), as well as during prior cold periods.

The study area is affected by a cold temperate climate, with significant E-W rainfall and temperature gradients that are associated with the presence of the Andes. Cyclones involving the Westerly winds originate in the polar front, creating high amounts of rainfall and low temperatures that directly affect the local climate (Garreaud, 2007). West of the SBMR, the annual precipitation reaches up to 10,000 mm in the accumulation zone of the SPIF (Cassasa et al., 2014), but further east (including the sector focused on here), the climate becomes drier and the annual precipitation only reaches 200 mm at Lago Argentino (Strelin et al., 2011). To the south of the SBMR, a weather station (<100 m altitude) at Torres del Paine records an annual precipitation of about 650 mm (Peña and Gutiérrez, 1992).

The SBMR, largely drained by the Baguales River, is located at 50°44' S and 72°24' W, and comprises part of the foothills of the Southern Patagonian Andes. In some parts of the SBMR the glacial cirques are developed over sedimentary rocks of the Eocene Man Aike Formation, a sequence of shales, sandstones and conglomerates with numerous mollusk fossils that overlies the Cretaceous Dorotea Formation and is, in turn, overlain by continental shales and sandstones rich in plant fossils belonging to the Río Leona Formation. The latter is followed by sandstones, conglomerates and mudstones of the Estancia 25 de Mayo and Santa Cruz Formations (Le Roux et al., 2010; Bostelmann et al., 2013). Gutiérrez et al. (2013) mentioned that the Estancia 25 de Mayo Formation is intruded by laccolith-type plutons and olivine-gabbro sills. In other parts of the SBMR, the glacial cirques are developed into these intrusive units.

2.2. Geomorphology

Previous studies discussed various aspects of the regional glacial geomorphology (Marden, 1997; Fogwill and Kubik, 2005; Glasser *et al.*, 2008; Strelin *et al.*, 2011; García *et al.*, 2012; Solari *et al.*, 2012). These studies show that between 50° and 51° S, the valleys distributed along the eastern margin of the SPIF contain moraine systems that indicate the action of effluent ice sheet outlet lobes and smaller glaciers flowing away from Andean divide. In contrast, we

focused on the SBMR where glacial cirques provide evidence of mainly an alpine (non-ice sheet) style of glaciation (Fig. 1). Using aerial photographs and satellite imagery, plus field observations, it is clear that glaciers still occupy some of the cirques in the SBMR and its surroundings. Glacial cirques have been subject to varied erosion processes (Fig. 2) as testified, for example, by the presence of mass wasting deposits on the cirque flanks and floors. Some cirques host remnants of ancient moraine-dammed lakes, and there is also evidence of eroded remnants of lateral moraines (Fig. 3), as well as faceted and striated blocks of different sizes (Fig. 4).

No direct age control for the last occupancy is available for the glacier cirques or the SBMR. However, we can establish a tentative framework for the chronology of glacial variations based on nearby studies. For cirques located near the current SPIF in areas covered by the Pleistocene ice sheet (Fig. 1), based on McCulloch et al. (2000); Sagredo et al. (2011) and Strelin et al. (2011), it is possible to infer that deglaciation started between ~17 and 15 ka. West of the SBMR, the southern Andes underwent substantial ice regrowth during the Late Glacial Interval or Antarctic Cold Reversal (ACR), from ~14 to 13 ka (Fogwill and Kubik, 2005; Moreno et al., 2010; Strelin et al., 2011). By implication, we infer that at least some cirques in the study area were re-occupied during the ACR. Subsequently, glaciers in the nearby Andes experienced repeated fluctuations throughout the Holocene (e.g., Strelin et al., 2014). We consider that the SBMR cirques, at least those currently occupied by ice, experienced similar variability. However, it remains unclear whether cirques without glaciers were reoccupied during the Holocene. Future studies will help to define the timing of cirque glacier activity throughout the study area and test the assumptions above.

3. Methodology

A total of 143 glacial cirques were identified and mapped. Mapping was carried out using the following (i) topographic maps at a scale of 1:50,000 (Portezuelo Baguales, Cerro La Mesa, Sierra Contreras) of the Chilean Instituto Geográfico Militar (IGM), (ii) aerial photographs at a scale of 1:70,000 obtained from the Servicio Aerofotogramétrico de la Fuerza Aérea de Chile (SAF). And (iii) Landsat imagery and digital elevation models (ASTERGDEM, with a resolution of 1 arc-second, and GMTDE2010, with

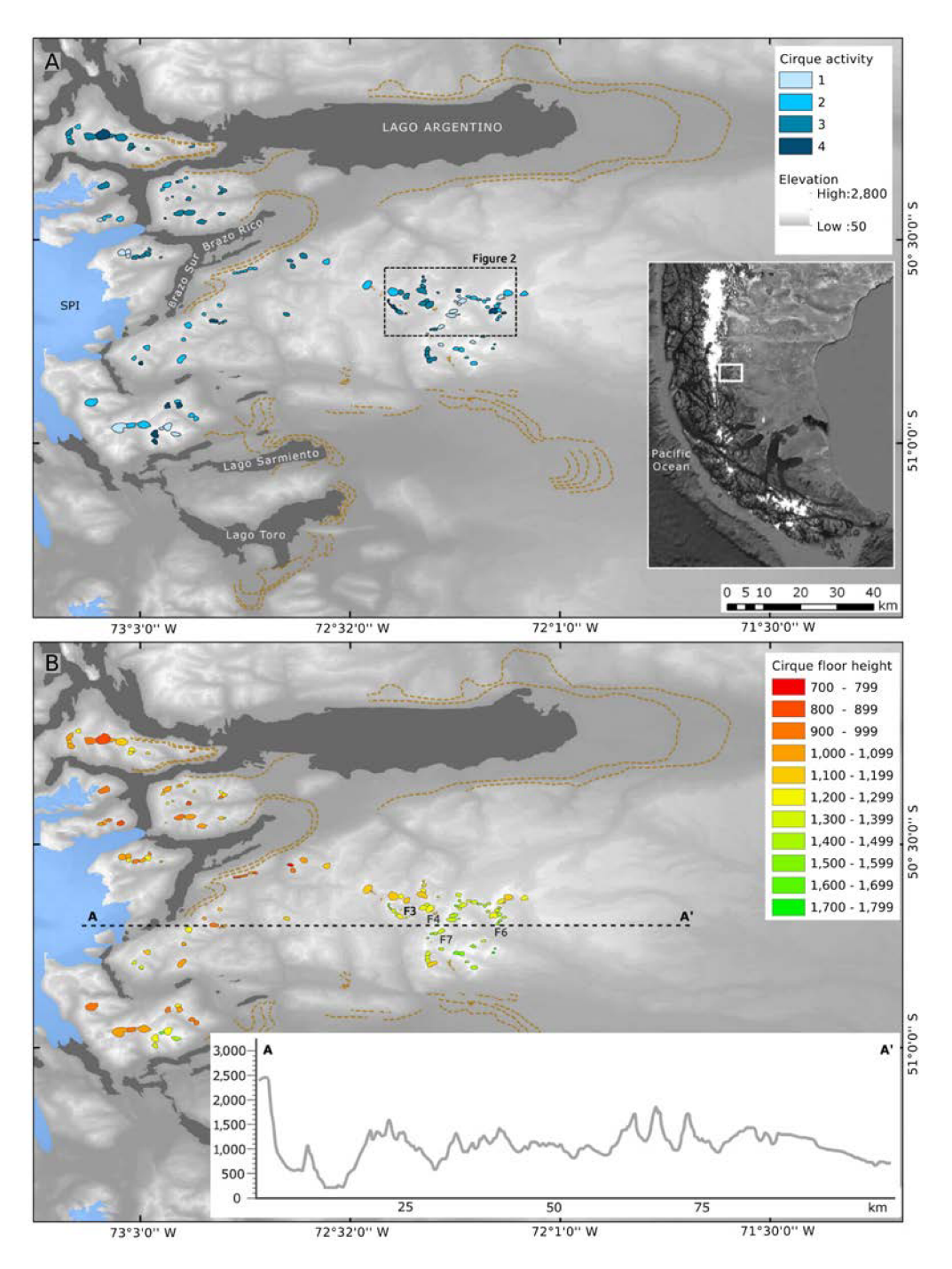


FIG. 1 **A.** Right box shows the location of the study area. Elevations were obtained from the SRTM model. The brown dotted line shows the major moraine systems east of Lago Argentino, Brazo Rico and Brazo Sur (Mercer, 1976; Strelin and Malagnino, 2000; and references therein), and south and east of Lago Toro and Lago Sarmiento respectively (Sagredo *et al.*, 2011; García *et al.*, 2012) these represent former outlet lobes during the LGM and prior glaciations. Cirque activity corresponds to **1.** current glacier activity; **2.** perennial snow activity; **3.** no glacier or snow activity; **4.** not categorized. Black dotted box shows SBMR area (Fig. 2). **B.**Mapped cirque floor elevations, which show the increase in elevation towards the east (from 700-799 m a.s.l. At east margin of SPIF, to 1,700-1,799 m a.s.l, on the eastern margin of SBMR). A-A' shows a topographic profile from SPIF to easternmost SBMR. F3, F4, F6 and F7 refer to figures that contain photos that show the position of the SBMR glacial features pictures.

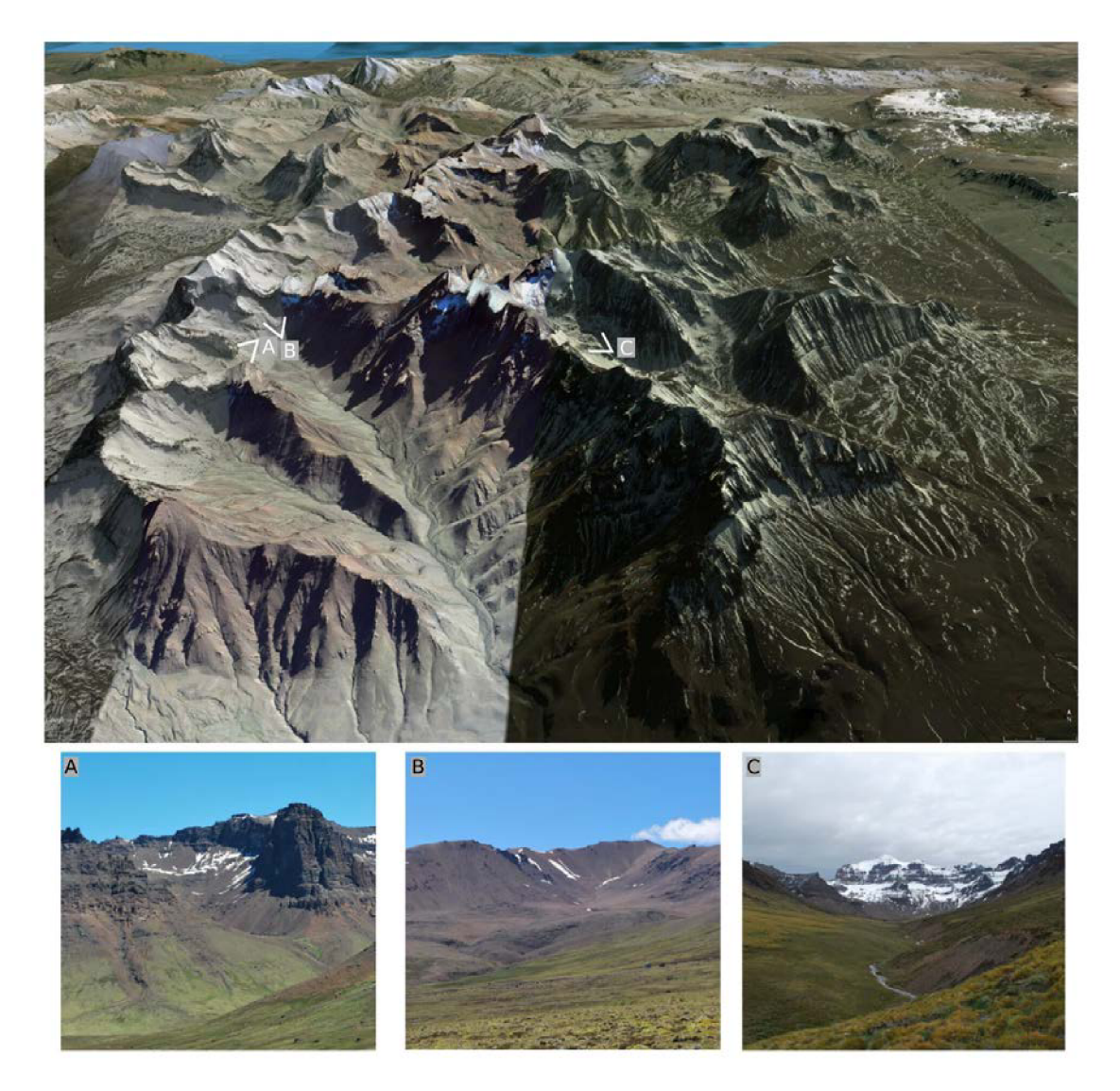


FIG. 2. Google Earth © image showing the study area from the SW. Photographs **A** and **B** (see location on Google image) show a hanging valley and glacial cirque, and photo **C** shows a glacial valley. Current snow and glacier processes are particularly active along the high elevations on the eastern side of the SBMR (*i.e.*, see figure 1).



FIG. 3. Lateral moraine (dotted gray line) below the cirques shown in figure 2A (location in figure 1B).



FIG. 4. Striated (white arrows) block (location shown in figure 1B).

a resolution of 7.5 arc-second) obtained from the USGS Earth Explorer website (http://earthexplorer. usgs.gov/ last visit 12-02-2018) (Table 1). Three field campaigns were carried out during 2013 and 2014 to map cirques and observe, describe and interpret the general geomorphology of the SBMR.

The identified cirques were digitized on satellite images and aerial photos. These were superimposed on ASTERGDEM and a slope map to provide a suitable topographic context, which is useful in identifying morphologies in areas with complex terrains (Horta *et al.*, 2013). The boundaries of the cirques were defined considering the criteria used by Evans and Cox (1995), Cossart *et al.* (2012), Křižek *et al.* (2012) and Barr and Spagnolo (2013). The crest-lines were considered as the upper limits of the cirques. Lower limits were marked, in some cases, by the crests of frontal moraines. However, for most of the cirques, the lower limit was considered

as the transition between the gentle slope of the cirque floor and an abruptly sloping valley below. Visible topographic features on the photographs, satellite images, and contour levels, were also considered in the definition of the cirque limits (Fig. 5). Otherwise, former glacier extensions are estimated based on the distribution of lateral and frontal moraines.

Each cirque was digitized as a closed polygon with a unique ID number, upon which a table containing associated morphometric information was generated. Calculations of planimetric and hypsometric indices (Křížek *et al.*, 2012) were conducted using the open source software Quantum GIS 2.2 and GRASS 6.0. The calculation of variables such as length and width of the cirques was performed in ArcView 3.2.

Following Delmas *et al.* (2013), morphometric variables were defined in such a way as to make them directly comparable with previous work on

TABLE 1. DATA SOURCE FOR CIRQUE MAPPING.

Data type	Total	Resolution (m)	Vertical accuracy (m)	Date
Aerial photos	12	4	<10	1998
Landsat 7	3	30	-	1999-2001
Landsat 8	2	15	-	2013
ASTER GLOBAL DEM	1	10	10-25	2011
GMTED2010	1	26-30	<10	2010

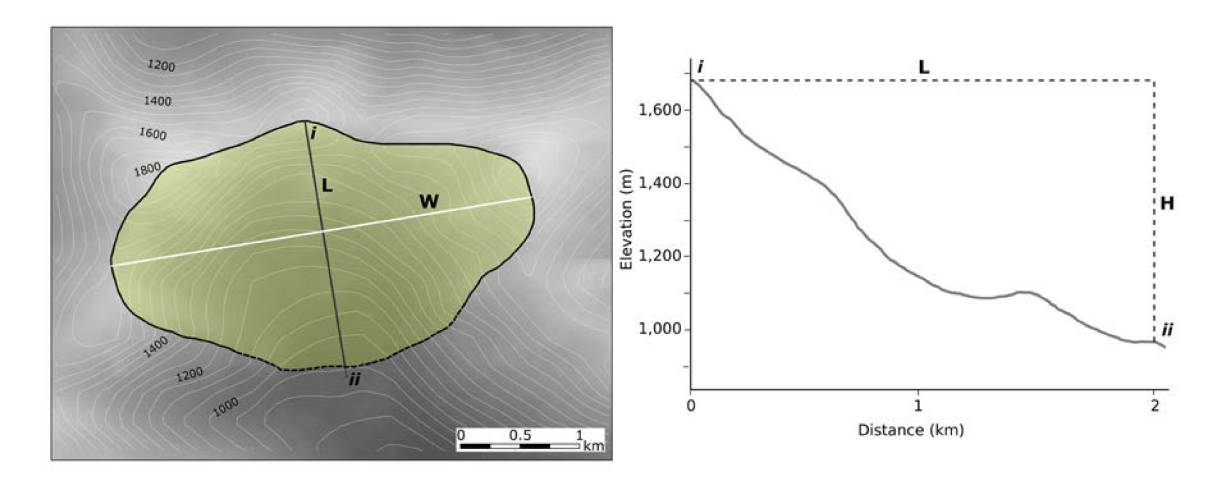


FIG. 5. Definition of key morphometric attributes of a hypothetical cirque. Left side shows the length (**L**) and azimuth (for aspect) as a black line and width (**W**) as a white line. **i-ii** correspond to a topographic profile based on elevation data obtained from ASTERGDEM. The right panel shows the characteristics of range (**H**) and the topographic profile i-ii.

glacial cirques located in middle and high latitudes around the globe (Evans and Cox, 1974; Aniya and Welch, 1981; García-Ruiz *et al.*, 2000; Federici and Spagnolo, 2004; Evans, 2006; Ruiz-Fernández *et al.*, 2009; Mindrescu *et al.*, 2010; Křížek and Milda, 2013; Delmás *et al.*, 2013; Gómez-Villar *et al.*, 2015). The variables considered are: surface (S_{fc}), perimeter (P), length (L), width (W), cirque depth (H), maximum elevation (E_{max}), mean elevation (E_{mean}), minimum elevation (E_{min}), aspect (A), ratio of length to elevation range (W/H), ratio of length to width (L/W), mean slope (S_{mean}), and circularity (C).

Surface (S_{fc}) corresponds to cirque area estimated in GIS, cirque length (L) was calculated as that of the mean axis line which passes through the midpoint of the cirque's lowest boundary (usually a moraine or a bedrock rim), and divides the surface of the cirque into two equal halves. The width (W) is the longest perpendicular line to the L axis (Federici and Spagnolo, 2004). The cirque depth (H) corresponds to the difference between the maximum elevation (E_{max}) , defined by the divide located immediately above the glacial cirque, and minimum elevation (E_{min}) measured in the lowest part of the cirque, coinciding most of the time with a narrowing between the lateral walls or with a glacial threshold (Aniya and Welch, 1981; García-Ruiz et al., 2000) (Fig. 5). Five altitudinal cirque classes were distinguished using the "Jenks" natural breaks classification method (Křížek and Milda, 2013), based

on a histogram of minimum cirque floor elevation (E_{min}): A (113-981 m a.s.l.), B (982-1,125 m a.s.l.), C (1,126-1,292 m a.s.l.), D (1,293-1,471 m a.s.l.), and E (1,472-1,741 m a.s.l.). Table 2 presents a summary of the morphometric characteristics of the cirques in the study area. The estimated elevation of morphometric parameters such as E_{max} , E_{mean} and E_{min} may present an error of ± 50 m, due to the horizontal and vertical resolution of DEMs (Table 1) and possible photo-interpretation errors.

The L/H ratio provides insight into the cross-sectional shape of the cirque, W/H describes the extent of the incision, and L/W indicates the planimetric shape of the cirque (Graf, 1976; García-Ruiz *et al.*, 2000; Gómez-Villar *et al.*, 2015). The values of maximum, medium and minimum elevation and slope (S_{mean}) were extracted from the ASTERGDEM using GIS tools (Křížek *et al.*, 2012). The aspect (A) was measured using the length axis orientation and expressed in radians (Křížek and Milda, 2013). The circularity (C) was obtained by dividing the perimeter of the cirque by the perimeter of a circumference of a circle that has the same area as the cirque (Aniya and Welch, 1981).

The L/W ratio was used to estimate former activity on cirques, as this parameter is considered to provide insight into the processes that affected their development. For example, cirques that are subject to erosion at their threshold by periglacial and fluvial processes after glaciations typically show L/W ratios <0.5; cirques that are or were

	Sfc (km²)	P (m)	L (m)	W (m)	E _{max} (m a.s.l.)	E _{mean} (m a.s.l.)	E _{min} (m a.s.l.)	H (m)	A (rad)	L/H	W/H	L/W	S _{mean}	С
Min	0.093	1,240	210	350	1,089	905	721	94	0.15	1.163	1.270	0.447	5.85	1.013
Mean	0.729	3,236	870	1,010	1,520	1,316	1,215	320	2.22	2.816	2.987	0.907	2.025	1.065
Average	0.983	3,481	960	1,095	1,554	1,332	1,216	339	2.44	3.086	3.473	0.920	21.10	1.075
Max	5.489	8,958	2,520	3,000	2,025	1,795	1,741	737	5.99	9.292	10.088	1.821	54.28	1.252
Sdev	0.893	1,518	422	514	214	198	208	145	1.20	1.383	1.503	0.248	7.27	0.039

TABLE 2. SUMMARY OF 143 CIRQUE MORPHOMETRIC CHARACTERISTICS.

 S_{fc} : Surface; P: Perimeter; L: Length; W: Width; E_{max} : Maximum elevation; E_{mean} : Mean elevation; E_{min} : Minimum elevation; H: Cirque depth; A: Aspect; L/H: Ratio of length to elevation range; W/H: Ratio of width to elevation range; L/W: Ratio of length to width; S_{mean} : Mean slope; C: Circularity.

extensively/solely occupied by a cirque glacier prior to deglaciation show 0.5<L/W ratios<1; and cirques that are or were extensively occupied by a valley glacier with a long ablation tongue show an L/W ratio>1 (Damiani and Panuzzi, 1987; Federici and Spagnolo, 2004; Steffanova and Mentlík, 2007). Also, erosion dominated by cirque-type glaciers should be greatest when Equilibrium Line Altitude (ELAs) are at or near the cirque floor height, which may occur during the initial stages of glaciation and during glacier retreat. On the other hand, cirque erosion may be minimal if the ELA lies below the cirque floor elevation and consequently glaciers grow into cirque-valley systems (Federici and Spagnolo, 2004; Steffanova and Mentlík, 2007).

Each parameter was analyzed in terms of its minimum, maximum and average values. Correlations between dependent (surface, perimeter, length, width, cirque depth, minimum elevation, mean slope and circularity) and independent (maximum elevation, aspect) morphometric variables were detected using Pearson correlation coefficients. The statistical significance was obtained using a t-test with a significance level of p=0.05. Morphologically similar cirque groups were identified by tree cluster analysis based on the Ward method and Euclidean distances (*sensu* Křížek and Milda, 2013).

For the first time in a cirque morphometric analysis, a composite map methodology (Le Roux and Rust, 1989; Merriam and Jewett, 1989; Le Roux, 1997; Sepúlveda *et al.*, 2013) was used to assist in the cirque characterization. This technique was originally designed for paleogeographic reconstructions and uranium exploration and is based on the combination of different parameters (characteristics of cirques in this case) into single, combined values, which

are eventually plotted on a composite map. The methodology has the advantage that for a specific data point, any number of different parameters pertaining to that location can be combined into a single, non-dimensional value, as long as the inherent meaning of the different parameters are understood. For example, if cirques are classified into two morphological types (1 and 2), type 1 may be characterized by a steep floor slope, small surface area, and small L/W ratio, whereas type 2 could have gentle slopes, large surface areas and high L/W ratios.

For the composite map, because the original parameters are expressed in different dimensions (degrees, km², and a dimensionless ratio), they cannot be combined unless they are first standardized into non-dimensional values with the same range. This is carried out as follows: As a first step, each parameter is allotted a standard percentage value (S) given by 100/n, where n is the number of morphometric attributes analyzed. In the case above, n=3, so that each parameter would have an S-value of 33.33. The range of numerical data of each parameter for all the different data points (individual cirques) in the study area is then standardized by using a conversion factor (C), given by $S/(G_b-G_1)$, where G_b and G_1 are the highest and lowest values of each parameter for all the cirques. If the slopes of the different cirques range between 2 and 15°, C would be 33.33/ (15-2)=2.5638. The numerical value G_1 of a specific parameter at each cirque is then converted by first calculating its transition value T, given by $(G_i - G_i)$, and then by multiplying T with the conversion factor C of the parameter.

The cirque with the lowest floor slope of 2° would thus have a *T*-value of (2-2)=0, whereas the cirque with the highest slope would have T=(15-2)=13. Therefore,

the first case would have a new dimensionless slope value of 0x2.5638=0, and in the second case, 13x2.5638=33.33. A circue with a 7° slope would have a standard value of 12.82. The other two parameters will also have a range of standardized, dimensionless values between 0 and 33.33, so that they can easily be combined. However, bearing in mind that type 1 cirques have high slopes but small surface areas and width/length ratios, the converted slope values (V) have to be inverted by subtracting them from S so that type 1 cirques are reflected by the lowest values of all three parameters. Therefore, for the cirque with the highest floor slope, the inverted slope value (I) would be 33.33-33.33=0, which would coincide with lower surface area and width/length ratio values of type 1 cirques.

Adding in this case the three standardized values discussed above for each cirque thus produces a dimensionless combined value (D_c) which reflects the type of cirque or transitions into other cirque types in an unbiased, objective manner. Specific cirques that fall in-between the two morphological classes defined above might have steep slopes and low surface areas but intermediate or high width/length ratios. However, they should still have a lower combined value than type 2 cirques, thus classifying

as type 1 cirques, if the combined value is less than 50. Transitional cirque types, with values between 33.33 and 66.66, can also be considered.

The composite values of all the cirque stations are finally plotted on a map and interpolated, in this case using the Inverse Weighted Distance (IWD) technique in ArcMap. This shows the spatial distribution of the cirque types.

4. Results

4.1. Cirque classification according to their activity

The interpretation of aerial photos, satellite imagery and field work allowed the identification of three cirque categories according to the presence/absence of snow or ice. These categories are distributed from the eastern margin of the SPIF, towards the interior of the continent to the easternmost section of the SBMR (Figs. 1, 2):

i) Cirques with current glacier activity (14.7%) (Fig. 6), which are mainly located in two areas: surrounding the SPIF (9 cirques) and around the eastern sector of the SBMR (12 cirques) at an average elevation of 1,395 m and 1,544 m, respectively, with a SE aspect bias.



FIG. 6. Cirque showing evidence of glacier activity, at the easternmost section of the SBMR (location in figure 1B).

- ii) Cirques with perennial snow activity (42%) (Fig. 7), distributed as follows: surrounding the SPIF (35 cirques), an intermediate zone, which corresponds to a topographic depression between the ice field and the adjacent mountain ranges, (6 cirques) and in the eastern sector of the SBMR (20 cirques) with an average elevation of 1,224 m, 1,081 m and 1,537 m, respectively. Aspects ranges are wide, from E to S.
- iii) Cirques with no glacier or perennial snow activity (28.7%) (Fig. 2 A, B), located in the vicinity of the SPIF (20 cirques), intermediate zone (4 cirques) and the eastern sector of the SBMR (17 cirques), at average elevations of 1,198 m, 1,061 m and 1,367 m respectively. These have a similar aspect as group ii) but with more of an E bias.

Finally, 14.6% (20 cirques) of the entire population was not classified due to a lack of adequate information because of image quality or coverage.

4.2. Cirque shape

Table 2 presents a summary of the morphometric characteristics of the cirques. Surface area values vary between 0.093 km² and 5.489 km², with an average value of 0.983±0.1 km². Their length ranges between 210 and 2,520 m, with an average value of 960±35m. The width varies between 130 and 3,000 m, with an average of 1,095±43 m. The frequency distribution of L, W and H are shown

in figure 8. Extreme values for S_{fc} , L and W are distributed geographically in two particular areas (Fig. 1): i) Eastern margin of the SBMR, where the smallest (also the shortest) cirques are located, at an average elevation of 1,700 m; ii) eastern margin of the SPIF, where the largest and widest cirques are located at an average elevation of 1,000 m. The spatial distribution of the cirque surface areas and shape parameters appear to be a function of the type of cirque activity, which we elaborate in the discussion.

The positive and statistically significant correlations between the shape parameters L and $S_{\rm fc}$ (0.905), and W and $S_{\rm fc}$ (0.935), shown in table 3, allow us to infer that circules tend to grow equally in both dimensions. This inference is further reflected by the average value of circularity (Table 2), 1.075, illustrating that those circules tend to maintain a naturally circular shape (Aniya and Welch, 1981).

4.3. Elevation, slope and aspect

Average elevations for $E_{\rm min}$, $E_{\rm mean}$ and $E_{\rm max}$ correspond to 1,216±17 m, 1,322±17 m and 1,554±18 m, respectively. As shown in table 3, $E_{\rm max}$ has a positive correlation with the elevation range, mean slope and parameters that define the shape of cirques ($S_{\rm fc}$, L, W). The correlation between $E_{\rm min}$ and cirque shape parameters is negative, which is particularly noticeable in the higher sections of the SBMR.



FIG. 7. Cirque showing perennial ice and snow activity (location in figure 1B). This photo was taken in early summer 2014.

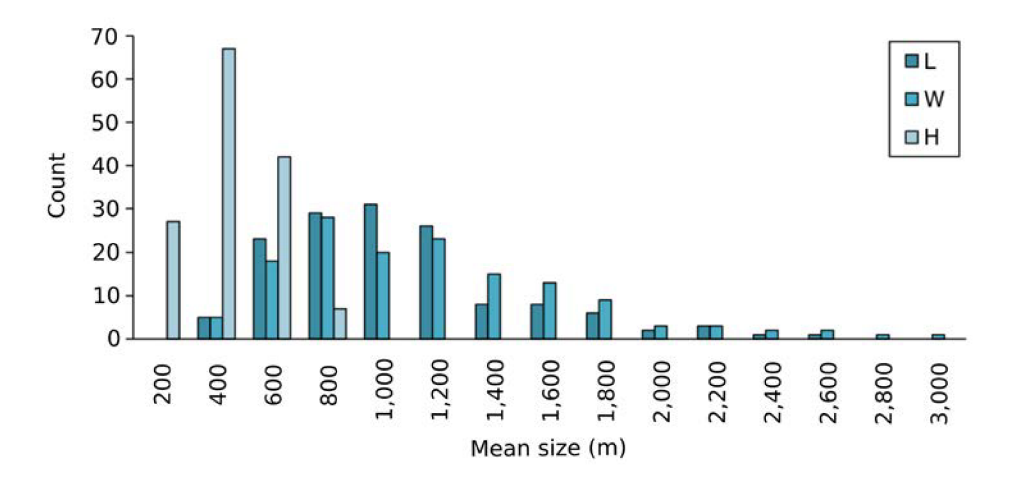


FIG. 8. Frequency distribution of L, W and H. Cirque mean surface (km²) decreases with an increasing in depth (H). Otherwise, when the average slope becomes gentle (*i.e.*, decrease of H), cirques are most likely to grow longitudinally and laterally. As shown in figure 1, large cirques are concentrated along the eastern margin of the SPIF and gradually get smaller towards the interior of the continent around the SBMR.

Slope values vary between 5.9° and 54.3° with an average value of 21.1±0.6°. Also slope shows a negative correlation with L/H and W/H ratios (Table 3), *i.e.*, the steeper the cirque, the smaller its size. Particularly at greater H, the cross-section and incision of cirques are reduced as the glacier occupied a smaller area thereof, which limited erosion; therefore, these cirques have lower surface areas. Otherwise, gentle slope cirques (*i.e.*, lower H) show larger surface areas and eroded floors.

Aspect values in radians vary in a range between 0.15 and 5.99, averaging 2.44±0.4, showing an E to SE bias (Fig. 9). Seventeen cirques (11.89%±1.4%) have aspect values between 0.2 and 5.3, showing WNW to NE aspects, while 37 cirques (25.87%±3.1%) are between 2.95 and 4.91, showing S to W aspects. Eighty-nine cirques, which represent 62.64% of the total, are between 0.98 and 2.95, showing a preponderant aspect of ENE to SSE. The aspect has a positive correlation with L and L/H attributes and a negative correlation with elevation parameters.

Table 4 shows a summary of cirque attributes by aspect. Larger cirques show aspects that range from SE to W, and are located in a wide elevation range, from B to E altitudinal classes (982-1,741 m a.s.l). Smaller cirques show aspects that range from SSE to N, and are located in higher sectors, mainly in altitudinal classes D and E (1,293-1,741 m a.s.l). Larger cirques show a gradual size increase moving from W to S aspects, and smaller cirques from N

to SW aspects. In both cases circularity decreases moving towards S-facing aspects, as here cirques tend to be longer than wider.

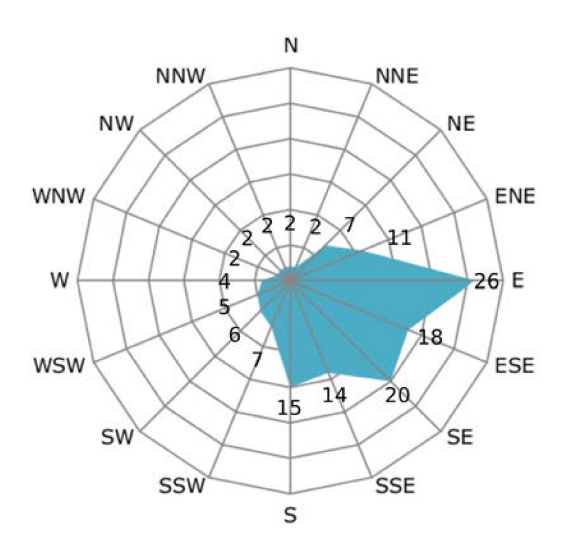


FIG. 9. Rose diagram showing frequency distribution of aspect. Cirques with a SW aspect tend to be located in the intermediate zone and altitudinal range E (1,472-1,741 m a.s.l), while cirques with S aspects are preferably located at the SPIF. Otherwise cirques with a S to SE aspect show a homogeneous distribution within the study area and an altitudinal range between C to D (1,126-1,292 and 1,293-1,471 m a.s.l.). Moreover cirques with W to SW aspects tend to show larger surface areas.

TABLE 3. CORRELATION BETWEEN ANALYZED MORPHOMETRIC CHARACTERISTICS.

	Sfc	P	L	W	E _{max}	E _{mean}	\mathbf{E}_{\min}	Н	A	L/H	W/H	L/W	S _{mean}	C
S_{fc}	1													
P	0.964	1												
L	0.905	0.919	1											
W	0.935	0.967	0.834	1										
$\boldsymbol{E}_{\text{max}}$	-0.009	0.011	0.003	0.031	1									
$\boldsymbol{E}_{\text{mean}}$	-0.279	-0.302	-0.278	-0.287	0.849	1								
\boldsymbol{E}_{\min}	-0.372	-0.403	-0.383	-0.375	0.764	0.960	1							
Н	0.520	0.593	0.554	0.582	0.379	-0.126	-0.307	1						
A	0.102	0.096	0.191	0.036	-0.157	-0.223	-0.268	0.153	1					
L/H	0.320	0.302	0.423	0.222	-0.358	-0.148	-0.066	-0.433	0.013	1				
W/H	0.414	0.412	0.320	0.450	-0.325	-0.154	-0.068	-0.381	-0.159	0.805	1			
L/W	-0.154	-0.192	0.137	-0.372	-0.115	-0.034	-0.026	-0.133	0.278	0.281	-0.293	1		
S _{mean}	-0.301	-0.293	-0.380	-0.227	0.361	0.167	0.086	0.410	-0.007	-0.789	-0.683	-0.262	1	
C	0.129	0.230	0.052	0.238	0.001	-0.108	-0.090	0.131	-0.116	-0.090	0.107	-0.277	-0.005	1

 S_{FC} , P, L, and W parameters have a high positive correlation followed by the altitude range (H). These variables are dependent and determine mainly the shape and cirque development. On the other hand, the E_{mean} , E_{min} and S_{mean} parameters have a weak negative correlation with the shape parameters. Particularly S_{mean} has a strong negative correlation with the planimetric development and cirque incision. See table 2 for definition of attributes.

TABLE 4. DISTRIBUTION OF CIRQUE ATTRIBUTES WITH ASPECT.*

	N	NNE	NE	ENE	E	ESE	SE	SSE	S	SSW	SW	WSW	W	WNW	NW	NNW
Count	2	2	7	11	26	18	20	14	15	7	6	5	4	2	2	2
S_{fc}	0.568	0.954	0.809	0.742	0.791	1.052	1.341	0.710	1.293	0.780	0.683	1.527	1.600	1.081	0.716	0.452
P	2,727	3,599	3,344	3,048	3,179	3,689	3,944	2,994	3,952	3,281	2,768	4,450	4,462	3,926	3,210	2,565
L	735	840	926	813	824	952	1,076	862	1,149	1,019	848	1,330	1,233	995	820	920
W	845	1,205	1,050	1,019	1,009	1,221	1,253	918	1,159	987	850	1,408	1,378	1,250	1,045	600
$\boldsymbol{E}_{\text{max}}$	1,824	1,415	1,574	1,634	1,619	1,567	1,577	1,539	1,361	1,373	1,663	1,469	1,595	1,806	1,598	1,451
$\boldsymbol{E}_{\text{mean}}$	1,610	1,246	1,411	1,458	1,410	1,305	1,312	1,315	1,172	1,144	1,465	1,225	1,314	1,459	1,413	1,273
\boldsymbol{E}_{\min}	1,506	1,123	1,308	1,351	1,302	1,209	1,194	1,198	1,054	1,005	1,312	1,073	1,155	1,283	1,296	1,216
Н	318	292	266	283	317	358	383	341	306	369	351	396	440	523	302	235
L/H	2.336	3.806	3.774	3.047	2.966	2.794	2.846	3.112	3.983	2.888	2.555	3.334	2.885	1.918	2.862	4.007
W/H	2.670	5.088	4.403	3.785	3.588	3.545	3.243	3.178	3.890	2.913	2.569	3.640	3.236	2.395	3.520	2.572
L/W	0.874	0.718	0.869	0.824	0.863	0.830	0.917	0.974	1.058	1.013	1.007	0.941	0.949	0.801	0.803	1.544
S _{mean}	22.550	17.535	16.986	21.282	23.312	20.864	20.528	23.807	16.283	20.057	25.527	20.372	23.473	26.525	20.910	14.865
C	1.038	1.062	1.094	1.063	1.086	1.090	1.076	1.062	1.072	1.066	1.049	1.061	1.074	1.077	1.074	1.077

^{*} See Table 2 for definition of attributes.

4.4. L/H W/H and L/W ratios

The highest L/H values are given by those cirques with NNW, NNE, NE, and S aspects. W/H values are higher in the NNE, ENE NE and S aspects. Considering this, cirques whose predominant aspect is NE, NNE and S, show broader cross section and deep incision (Table 4).

The descriptive L/W ratio can also be used for classifying cirques according to their former activity (Damiani and Panuzzi, 1987; Federici and Spagnolo, 2004; Steffanova and Mentlík, 2007). In the case of the SBMR, 64% of cirques were occupied for the most part by cirque-type glaciers, while 34% of the cirques flowed into valley glaciers. About 1% of the cirque topography was deeply affected by post-glacial processes such as rock weathering, landslides and deposition. This is consistent with landform preservation, including cirques and alpineglaciated topography, in the arid rain shadow of the Andes (Rabassa *et al.*, 2011).

4.5. Morphological cirque types

Based on cluster analysis, two morphological cirque types can be distinguished (Fig.10, Table 5). They differ mainly in their surface and shape parameters (S_{fc}, L, W). Type 1, located at the eastern margin of the SPIF and mainly in the higher areas of the SBMR, has a mean surface area of 0.361 km² (644 m length and 668 m width), while Type 2, broadly distributed over the study area, has a mean area of 1.487 km² (1,215 m length and 1,440 m width). Both types show a similar overall aspect distribution with a S to E bias and a similar mean slope.

Morphological Type 1 shows a cirque floor average elevation of 1,273 m, and these usually show current glacial activity. On the other hand, morphological Type 2 shows a cirque floor average elevation of 1,169 m, and usually contains either perennial snow or a lack of snow/ice activity (possibly due to their lower elevation).

Spatial distribution of cirques type could be related to the presence of the Andean massif, and regional precipitation gradient across 51° S, in addition to the contrast between massive glaciations towards the west, versus isolated and constrained to the Andean foothills glaciations, to the east of the study area.

4.6. Composite map

Composite values of the ten parameters considered, vary between 39.80 and 82.47 (Fig.11). The high values are related to cirques that show current glacier or perennial snow activity (Figs. 6, 7), where the predominant aspects range from E to S. These cirques are spatially concentrated in the highest sections (altitudinal cirque classes D and E, 1,293-1,741 m a.s.l) of the eastern SPIF and along the high elevations of the eastern side of the SBMR. Particularly for this case, cirque activity would be linked to topographical effects (rain shadow) and local weather conditions (temperature descent), which favor snowfall.

Low values are associated with cirques that show no evidence of present-day glacier or perennial snow activity (e.g., Fig. 2A, B). These cirques have aspects that range from NW to NE and show a broad spatial distribution at lower elevations (altitudinal cirque classes B and C).

The current cirque activity is mainly controlled by elevation and aspect. On the one hand, the higher elevation enables the development of snow and/ or ice activity, particularly in cirques with a gentle slope (S_{mean}) determined by a narrow elevation range (H), which favors snow accumulation. On the other hand, the cirque aspect can favor the persistence of ice or snow coverage, especially if oriented E to SE, due to the effect of lower solar radiation during the warmest part of the day and lower direct sunlight in the afternoon; this effect has already been described in Evans (1977), Evans and Cox (1995), Garcia-Ruiz *et al.* (2000), and Mindrescu *et al.* (2010).

5. Discussion

The glacial cirques development in the SBMR result from the combination of several climatic and non-climatic variables (Delmas *et al.*, 2013; Křížek and Milda, 2013; Ruiz-Fernández *et al.*, 2009; Evans, 2006; Federici and Spagnolo, 2004). The relative importance of these variables is difficult to rank. Previous studies have concluded that, based on glacial morphometry, it is difficult to establish clear relationships between independent (environmental factors) and dependent (size and shape of the cirques) variables due to the structural and lithologic complexity of mountain environments. For example, Aniya and Welch (1981) inferred that the morphological differences between cirques may

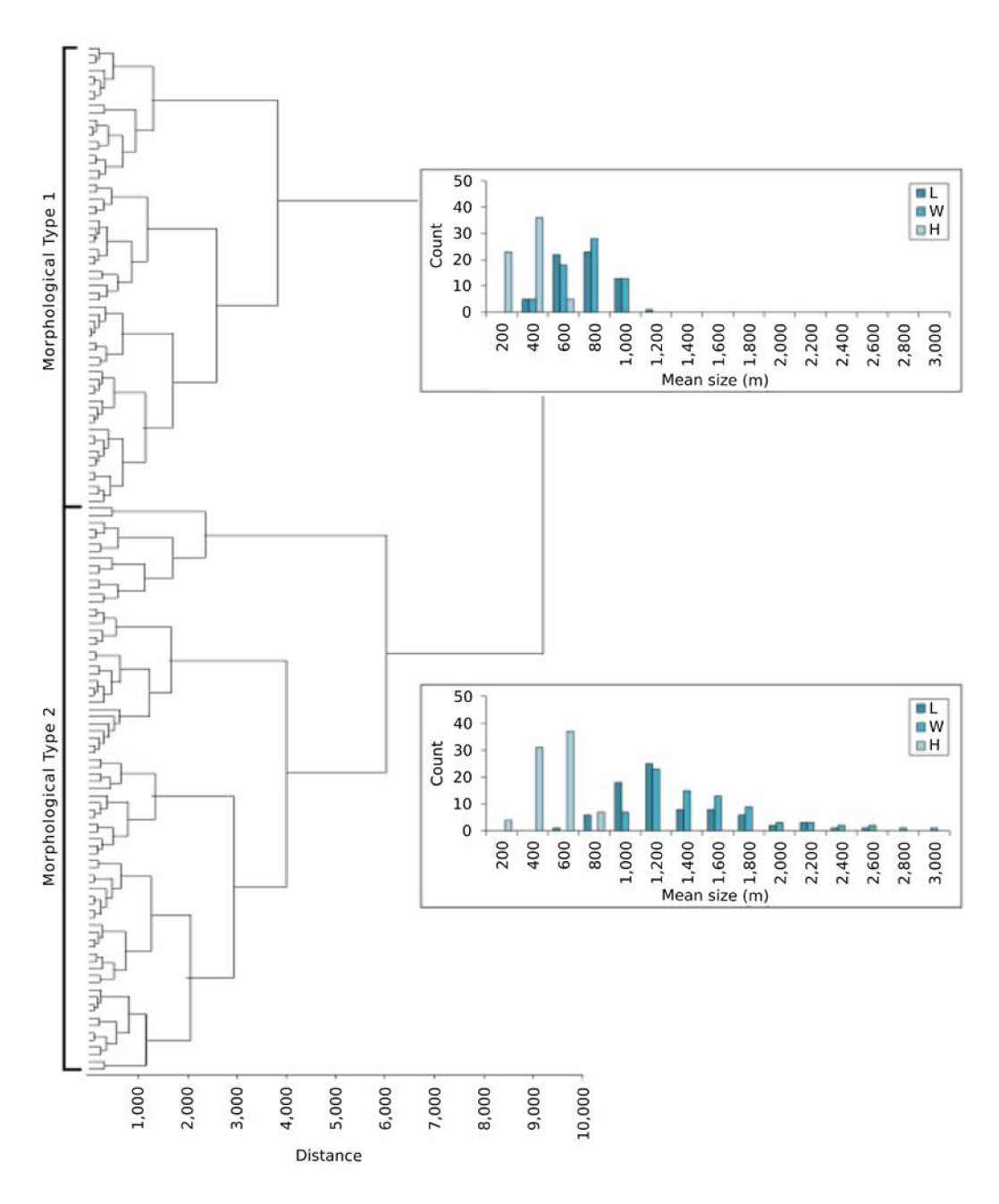


FIG. 10. Tree cluster of cirques (Euclidean distance measurements and amalgamation conducted by Ward's method). The analysis shows two major morphological Types where the differences are based on the cirque activity (*i.e.*, glacial, perennial snow, or absence of both), surface, shape and spatial distribution. Morphological Type 2 tends to show the largest cirques compared with the morphological Type 1.

reflect stages in the cirque development rather than differences in environmental factors. In our opinion the difficulty in separating long and complex histories of cirques evolution from the isolated influences of factors such as altitude, lithology and exposure can be overcome –at least in part– by using statistical analysis to estimate overall relations (*sensu* Ruiz-Fernández *et al.*, 2009).

		Type 1 (64	cirques)	Type 2 (79 cirques)						
	Mean	Median	Standard Deviation	Mean	Median	Standard Deviation				
S _{fc}	0.361	0.347	0.153	1.487	1.206	0.927				
P	2,209	2,203	0.496	4,511	4,307	1,264				
L	644	650	179	1,215	1,110	389				
W	668	680	161	1,440	1,320	436				
E _{max}	1,521	1,504	228	1,581	1,563	199				
E _{mean}	1,364	1,350	224	1,305	1,281	172				
E_{min}	1,273	1,288	237	1,169	1,175	169				
Н	248	235	99	413	410	134				
A	2.51	2.31	1.25	2.38	2.17	1.16				
L/H	2.836	2.596	0.949	3.288	2.906	1.632				
W/H	2.993	2.731	1.102	3.863	3.172	1.670				
L/W	0.990	0.952	0.272	0.863	0.830	0.212				
S _{mean}	22.668	21.460	7.531	19.824	19.090	6.835				
C	1.064	1.057	0.032	1.083	1.075	0.042				

TABLE 5. SUMMARY STATISTICS OF MORPHOMETRIC CHARACTERISTICS FOR CIRQUE TYPES OBTAINED FROM CLUSTER ANALYSIS. SEE TABLE 2 FOR DEFINITION OF ATTRIBUTES.

The spatial and morphometric analysis of glacial cirques located around 50° S, allows us to infer that the development and shape of most of the glacial cirques were controlled mainly by their aspect (i.e., exposure to solar radiation and Westerly winds) and cirque floor slope. In comparative terms, most of the glacial cirques of SBMR shares similar characteristics (less than 2 km for L and W, and less than 1 km for H), in particular with the glacial cirques located at Mt. Smolikas and Mt. Vasilitsa, in northwest Greece, (Hughes et al., 2007), in the Cantabrian Range in Spain (Ruiz-Fernández et al., 2009), Spanish Pyrenees (García-Ruiz et al., 2000), and in the Bohemian Massif in the Czech Republic (Křížek and Milda, 2013). The overall morphology and special distribution of the cirques in these relative well-studied European locations have been interpreted as predominantly controlled by lithology and geological structure, while for cirques development factors such as aspect and elevation are considered as the preponderant.

For both SBMR and northwest Greece, aspect is a determining factor in the cirque's development, wich can lead to larger and eroded examples, mainly at a southern aspect. However, cirque elevation effects are diverse. For SBMR, the Bohemian Massif, and Spanish Pyrenees, an increase in elevation can lead to a reduction in cirque size. Whereas for the

Cantabrian Range an increase in elevation determines an increase in cirque size. The elevation effect for cirques should be linked to controlling factors such as lithology and the geological structure of these massifs, as well as their spatial distribution in relation to moisture sources, Specially in the SBMR where the Westerly winds and associated climate systems and rainfall gradients play an important role in the cirques development, as we explain below.

In general, the spatial distribution of different cirques types in SBMR would be the result of the combined actions of the following: first the tectonic setting (Patagonian Andes uplift during the most recent stage of the Andean tectonic cycle –14 Ma–(Ramos and Ghiglione, 2008) and second the climatic pattern (Patagonian west-east climate contrast, which prevailed since the LGM), that sets a transition in glaciation types, from ice sheet glaciation near the Pacific coast in the west (maritime and temperate climate setting), to alpine glaciations in the east, in the higher sectors of the SBMR (dry and cold).

Tectonic uplift of the SBMR (14 Ma) set up an orographic barrier, and a significant E-W rainfall and temperature gradient. Actually, west of the study area, around the accumulation zone of the SPIF, the annual precipitation reaches up to 10,000 mm (Cassasa *et al.*, 2014), favoring the development of larger cirques also eroded by outlet glaciers from

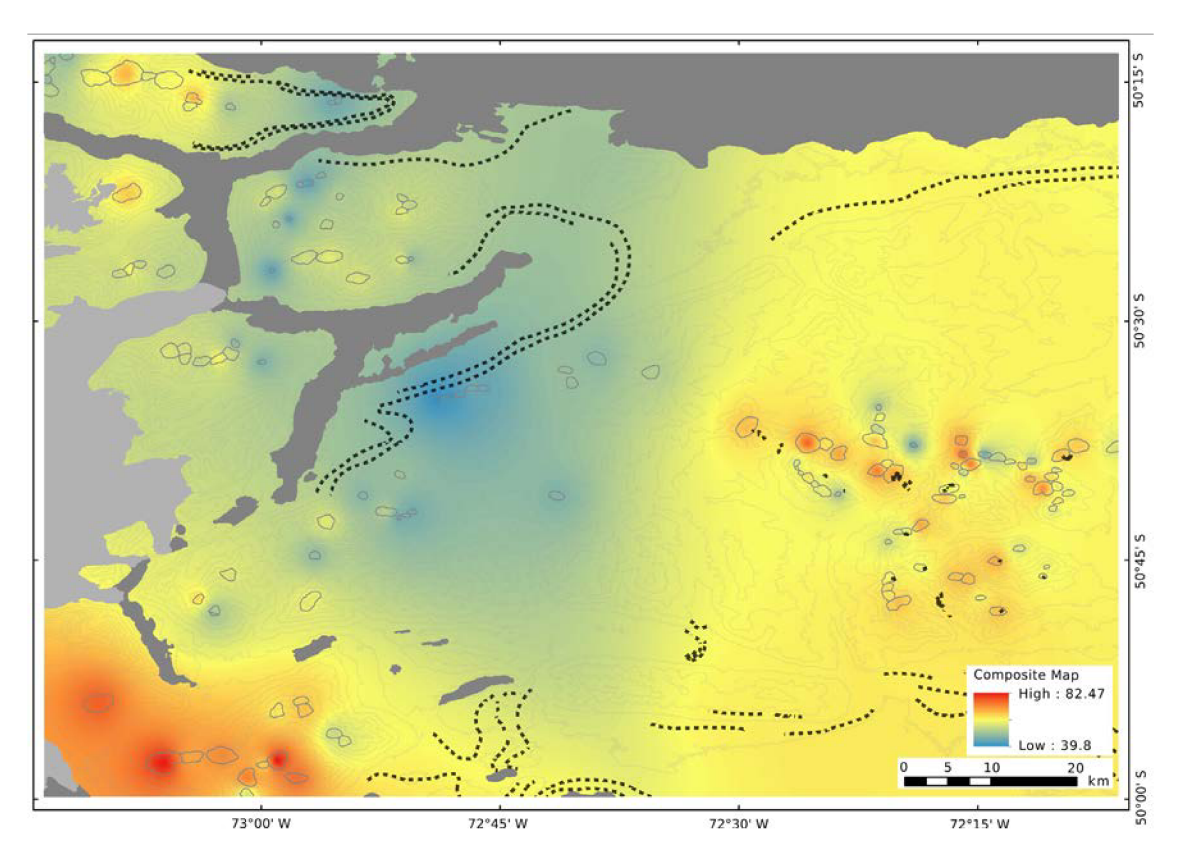


FIG. 11. Composite map of cirque attributes in the study area. Cirques were categorized using 10 parameters extracted from the morphometric analysis (Table 2). Black dotted lines show outlines of maximum extension glacier stages (see text). Areas with cirques closest to the SPIF, such as in the far SW, were partly covered or adjacent to the large ice sheet during the LGM (García et al., 2012; Strelin et al., 2011). This contributed to their higher areal development in relation to those located in the SBMR, which were isolated from the ice sheet outlet lobes. Note that high values (orange-red) show the spatial distribution of currently active snow/ice processes, which particularly for the Sierra Baguales, are conditioned by cirque floor elevations (Fig. 1) and the rainshadow effect. The lowest values (blue) spatially match with evidence of areas covered or adjacent to former outlet glaciers of the SPIF, and cirques with no evidence of current glacier or snow activity.

the Patagonian Ice Sheet (cirques Type 2). Farther east, the climate becomes drier and the annual precipitation varies from ~650 mm at Torres del Paine, to ~250 mm at Cerro Guido. We assume this reflects the rainfall gradient at SBMR, which favors the development of small cirques eroded by alpine-type glaciers (cirques Type 1), prevails at eastern higher areas of SBMR mainly due to the low temperatures associated with the E-W thermal gradient, moreover Type 1 reflects an alpine glaciated landscape that is isolated from coverage by the Pleistocene Ice Sheet, a particular morphoclimatic domain mainly in this eastern Andes foothills which also provides a useful natural laboratory for the study of the past environmental changes.

Another important factor in the development of the SBMR morphoclimatic configuration corresponds to the difference in the cirques floors elevations (cirques Type 1, is about 100 m above the cirques Type 2). The elevation factor helps the development of cirques that are extensively or commonly occupied by valley glaciers with a long ablation tongues that may have been influenced by activity associated with outlet glaciers from the Pleistocene Ice Sheet when it existed. As well, cirque floor elevation also influences the development of glacial activity east of the Andean foothills (along with ice sheet outlet glaciers) due to the temperature gradient at SBMR. That is whether they are currently occupied by remnant glacial activity, and their location and

size is mainly controlled by the low temperatures prevailing towards the interior of the continent. For large circues located just to the east of SPIF glacial activity also is influenced by the effect of high precipitation, near the Pacific coast.

5.1. Cirque distribution, elevation and dimensions

Based on the spatial distribution of the glacial cirques morphological types it is possible to recognize two domains of glacial activity in the study area. The first includes cirques Type 1 which mainly show evidence of perennial snowy activity, and in some cases evidence of glacial activity. Some of these cirques contain latero-terminal moraines, and are distributed in an elevation range from 1,395 to 1,554 m. On average, these elevations appear to be about 180 m above the altitude limit of landforms marking the expansion of the SPIF (into the Southern Patagonian Ice Sheet) during glacial maximun. The second includes cirques Type 2 that shows no evidence of current glacial or snow activity and is found at relatively low elevations ranging from 1,198 to 1,367 m, as we move from the SPIF region to the east.

Glacial deposits can also be considered as evidence of these glaciation limits. On the one hand morphological Type 1 can be linked to lateral moraine deposits constrained to the cirques (Figs. 3 and 7), while morphological Type 2 can be linked to ample moraine belts associated to Holocene maximum glacier extension (brown dotted line In Fig. 1, black dotted line in figure 9).

5.2. Paleoglacial significance

Topographic and climatic conditions, besides the west to east climate contrast across Patagonia (Glasser et al., 2008), were reflected in the extent and dynamics of Ice Sheet and outlet glaciers during the LGM and subsequent deglaciation (McCulloch et al., 2000; Sagredo et al., 2011, and Strelin et al., 2011). Western Patagonian Ice Sheet glaciers exhibited a highly dynamic behavior, in part due to high precipitation and a positive mass balance (Hulton et al., 2002), which favored the development of ice sheet glaciations associated with outlet lobes or glaciers. These outlet glaciers occupied the valleys located west of the SBMR, and east of the present-day SPIF. As soon as the large ice sheet outlet glaciers retreated to the west of the study area, due to an uninterrupted climatic change (i.e., prior to the Late Glacial; Marden, 1997; McCulloch *et al.*, 2000; Sagredo *et al.*, 2011; Strelin *et al.*, 2011; García *et al.*, 2012), the higher parts of the SBMR region could have became dominated by only cirque-type glaciers that prevailed because of sufficiently high elevations and cold enough pre-Holocene temperature conditions (Garreaud, 2007; Villa-Martínez and Moreno, 2007; Moreno *et al.*, 2009). However, our results indicate that the evolution of cirques in the study area was not uniform. Most likely because of a climatic gradient, cirque glaciers Type 2 developed to the west, near the SPIF, were more dynamic, and therefore their cirques experienced more erosion and enlarged more, than those to the east.

Differences in area and shape parameters of morphological types recognized in this study would be linked to the geographical evolution and climate of the study area, as well as aspect, exposure to the Westerly winds, and elevation. Morphological Type 1 cirques, mainly located at altitudinal classes D and E (1,293-1,741 m a.s.l), represent cirques that experienced glacial processes that persisted during the Holocene. Isolated from the SPIF during the Holocene, and under cold and dry weather conditions towards the interior of continent, this favored the presence of snow and ice coverage controlled mainly by aspect and local topographic conditions (Figs. 1, 11). Morphological Type 1 can also be associated with high composite values (Fig. 11), linked to the rain shadow related mainly to SBMR topography and temperature gradient which can favor snowfall.

On the other hand, morphological Type 2 cirques, mainly located at altitudinal classes B and C (982-1,296 m a.s.l), and grouped close to the SPIF as shown in the composite map (Fig. 11), most likely experienced higher precipitation and temperature, that would have caused that their glaciers to be more erosive (Barr and Spagnolo, 2015). Morphological Type 2 are related with low composite values (Fig. 11), linked to past outlet glacial activity associated with the Pleistocene Patagonian Ice Sheet. The outlet glaciers may have overrun and occupied these cirques, or they may have co-existed with the waxing and waning of glaciers in the cirques, which may have flowed into the valleys and merged with the lower larger ice masses.

Considering the above, we concluded that the morphological Type distribution (Fig. 11) indicates that the proximity to the SPIF has played a key role in the development of the cirques. This could be related

to the specific climatic gradient across the region. In particular, it is plausible that the larger cirques near the SPIF were more dynamic due to high ice flux facilitated by higher winter precipitation and summer temperatures (*sensu* Barr and Spagnolo, 2015) than the smaller cirques to the east. The latter hypothesis is consistent with the present-day precipitation gradient across the study area.

6. Conclusions

Tectonic uplift of the SBMR (14 Ma) allowed paleogeographic changes to take place east of the Main Andean Range. Given the Westerly winds and associated climate systems, SBMR tectonic uplift allowed intensification of the orographic effect, and associated temperature and precipitation gradients, which favored the development of independent alpine glaciers to the east even at relatively low elevations (1,293 to 1,741 m). This defined a new morphoclimatic setting in southern Patagonia, the Sierra Baguales alpine glaciated region, which can be considered as a satellite of the SPIF (Mercer, 1976). Glacier variations associated with this domain have hardly been studied, and represent an opportunity to assess and interpret those factors that enabled the development of individual, small and independent glaciations, which provide a sensitive proxy of past environmental changes in the eastern foothills of the Southern Andes.

Based on 14 morphometric parameters and morphological classification of the SBMR glacial cirques, as well as the development of a composite map, in which the morphometric parameters were combined and standardized, we infer two glaciation domains related to the climatic and glacial history that characterize the study area. The lower domain, located mainly in an intermediate zone between the eastern margin of the SPIF and lower sections of the SBMR (982 to 1,292 m, at altitudinal classes B to C), contains cirques that do not show current evidence of perennial snow activity or glacial processes. The surface and shape of these cirques suggest that they were highly dynamic, i.e., experienced comparatively higher erosion than other cirques in the region. The upper limit, particularly around the eastern side of the SPIF and in the most elevated sectors (1,293 to 1,741 m, altitudinal classes D to E) contains cirques that mainly show perennial snow activity followed by glacial processes and in some cases, remnants of latero-terminal moraines marking larger former alpine glaciers. The surface and shape of these cirques could be influenced by the action of alpine glaciers that persisted throughout the Holocene, due to prevailing low temperature and humidity conditions at the sites.

Along with the climatic gradient, other factors that favored the development of alpine-type cirque glaciations, including also the current glacial activity, that exists mainly around the upper level of the SBMR, include cirque floor elevation, mean slope, aspect and orientation (aspect) relative to the Westerly winds. Cirques located in the highest sections of the SBMR had favorable conditions for the development of snow and/or ice activity, due to the thermal gradient, specifically cool temperatures at the sites. Finally, if the cirque floor had a gentle slope this favored accumulation processes, and cirques with an easterly aspect favored the persistence of ice and/or snow cover due to low solar radiation during the warmest part of the day and less direct sunlight in the afternoon.

Acknowledgements

We are grateful for grants from the "Becas de Doctorado en Chile" Scholarships Program and "Gastos Operacionales para Proyecto de Tesis Doctoral" of CONICYT. J. MacLean and his family kindly allowed access to the farms Las Cumbres and Baguales and J.P. Riquez allowed access to the farm Verdadera Argentina. J.C. Aravena and R. Villa-Martínez of the Universidad de Magallanes, J.L. Oyarzún, and J.J. San Martín provided much-appreciated logistical support. R. Arce, M. González, and C. Peltier lent invaluable assistance in field activities. Kaplan issupported by NSF BCS 1263474, and in part by the Climate Center of LSEO and NASA GISS, and Le Roux by Project CONICYT/FONDAP/15090013. This is LDEO contribution 8252.

References

Aniya, M.; Welch, R. 1981. Morphometric analyses of Antarctic cirques from photogrammetric measurements. Geografiska Annaler, Series A: Physical Geography 63 (1/2): 41-53.

Barr, I.; Spagnolo, M. 2013. Palaeoglacial and palaeoclimatic conditions in the NW Pacific, as revealed by a morphometric analysis of cirques upon the Kamchatka Peninsula. Geomorphology 192: 15-29.

Barr, I.; Spagnolo, M. 2015. Glacial cirques as palaeoenvironmental indicators: their potential and limitations. Earth-Science Reviews 151: 48-78.

- Bostelmann, J.; Le Roux, J.P.; Vásquez, A.; Gutiérrez, N.; Oyarzún, J.; Carreño, C.; Torres, T.; Otero, R.; Llanos, A.; Fanning, M.; Hervé, F. 2013. Burdigalian deposits of the Santa Cruz Formation in the Sierra Baguales, Austral (Magallanes) Basin: Age, depositional environment and vertebrate fossils. Andean Geology 40 (3): 458-489. doi: 10.5027/andgeoV40n3-a04.
- Casassa, G.; Rodríguez, J.; Loriaux, T. 2014. A new glacier inventory for the Southern Patagonia Icefield and areal changes 1986-2000. *In Global Land Ice Measurements* from Space. Springer: 639-660. Berlin.
- Cossart, E.; Fort, M.; Bourlès, D.; Braucher, R.; Perrier, R.; Siame, L. 2012. Deglaciation pattern during the Late Glacial/Holocene transition in the southern French Alps. Chronological data and geographical reconstruction from the Clarée Valley (upper Durance catchment, southeastern France). Palaeogeography, Palaeoclimatology, Palaeoecology 315-316: 109-123.
- Charrier, R.; Pinto, L.; Rodríguez, M. 2007. Tectonostratigraphic evolution of the Andean orogen in Chile. *In* The Geology of Chile. The Geological Society Publishing House. Bath: 21-115. UK.
- Damiani, A.; Panuzzi, I. 1978. Carta di geomorphologia dinamica in funzione dela pianificazione territoriale. Bollettino Servizio Geologico Italia XCIC: 77-84.
- Delmas, M.; Gunnell, Y.; Calvet, M. 2013. Environmental controls on alpine cirque size. Geomorphology 206: 318-329.
- Diraison, M.; Cobbold, R.; Gapais, D.; Rossello, A.; Le Corre, C. 2000. Cenozoic crustal thickening, wrenching and rifting in the foothills of the southernmost Andes. Tectonophysics 316 (1-2): 91-119.
- Evans, B. 1977. World wide variations in the direction and concentration of cirque and glacier aspects. Geografiska Annaler, Series A: Physical Geography 59 (3): 151-175.
- Evans, B.; Cox, N. 1995. The form of glacial cirques in the English Lake District, Cumbria. Zeitschriftfür Geomorphologie 39 (2): 175-202.
- Evans, I. 2006. Allometric development of glacial cirque form: Geological, relief and regional effects on the cirques of Wales. Geomorphology 80 (3-4): 245-266.
- Evans, I.; Cox, N. 1974. Geomorphometry and the operational definition of cirques. Area 6 (2): 150-153.
- Federici, P.; Spagnolo, M. 2004. Morphometric analysis on the size, shape and areal distribution of glacial cirques in the Maritime Alps (Western French-Italian Alps). Geografiska Annaler, Series A: Physical Geography 86 (3): 235-248.
- Fogwill, C.; Kubik, P. 2005. A glacial stage spanning the Antarctic Cold Reversal in Torres del Paine (51° S), Chile, based on preliminary cosmogenic exposure ages.

- Geografiska Annaler, Series A: Physical Geography 87 (2): 403-408.
- García, J.; Kaplan, M.; Hall, B.; Schaefer, J.; Vega, R.; Schwartz, R.; Finkel, R. 2012. Glacier expansion in southern Patagonia throughout the Antarctic Cold Reversal. Geology 40 (9): 859-862.
- García-Ruiz, J.; Gómez-Villar, M.; Ortigosa, L.; Marti-Bono, C. 2000. Morphometry of glacial cirques in the central Spanish Pyrenees. Geografiska Annaler, Series A: Physical Geography 82 (4): 433-442.
- Garreaud, R. 2007. Precipitation and circulation covariability in the extratropics. Journal of Climate 20: 4789-4797.
- Glasser, N.; Jansson, K.; Harrison, S.; Kleman, J. 2008. The glacial geomorphology and Pleistocene history of South America between 38°S and 56°S. Quaternary Science Reviews 27 (3-4): 365-390.
- Gómez-Villar, A.; Santos-González, J.; González-Gutiérrez, R.B.; Redondo-Vega, J.M. 2015. Glacial cirques in the southern side of the Cantabrian Mountains of southwestern Europe. Geografiska Annaler Series A Physical Geography 97 (4): 633-651. doi: 10.1111/geoa.12104.
- Graf, W. 1976.Cirques as glacier locations. Arctic and Alpine Research 8 (1): 79-90.
- Gutiérrez, N.; Le Roux, J.P.; Bostelmann, E.; Oyarzún, J.; Ugalde, R.; Vásquez, A.; Otero, R.; Araos, J.; Carreño, C.; Fanning, M.; Torres, T.; Hervé, F. 2013. Geology and stratigraphy of Sierra Baguales, Última Esperanza province, Magallanes, Chile. Bolletino di Geofisica Teorica ed Applicata 54: 327-330.
- Horta, L.; Busnelli, J.; Georgieff, C.; Aschero, C. 2013. Landform analysis of the Pueyrredón Lake area in northwestern Santa Cruz, Argentina. Quaternary International 317: 19-33.
- Hughes, P.; Gibbard, P.; Woodward, J. 2007. Geological controls on Pleistocene glaciation and cirque form in Greece. Geomorphology 88 (3-4): 242-253.
- Hulton, N.; Sugden, D.; Payne, A.; Clapperton, C. 1994. Glacier modeling and the climate of Patagonia during the Last Glacial Maximum. Quaternary Research 42 (1): 1-19.
- Hulton, N.; Purves, R.; McCulloch, R.;Sudgen, M.; Bentley, M. 2002. The Last Glacial Maximum and deglaciation in southern South America. Quaternary Science Reviews 21: 233-241.
- Kaplan, M.; Hein, A.; Hubbard, A.; Lax, S. 2009. Can glacial erosion limit the extent of glaciation? Geomorphology 103: 172-179.
- Křížek, M.; Milda, P. 2013. The influence of aspect and altitude on the size, shape and spatial distribution of glacial cirques in the High Tatras (Slovakia, Poland). Geomorphology 198: 57-68.

- Křížek, M.; Vočadlová, K.; Engel, Z. 2012. Cirque overdeepening and their relationship to morphometry. Geomorphology 139-140: 495-505.
- Le Roux, J.P. 1997. Palaeogeographic reconstructions using composite maps, with the case studies from three continents. Palaeogeography, Palaeoclimatology, Palaeoecology 131: 51-63.
- Le Roux, J.P.; Rust, I. 1989. Composite facies map: a new aid to palaeo-environmental reconstruction. South Africa Journal of Geology 92: 436-443.
- Le Roux, J.P.; Puratich, J.; Mourgues, A.; Oyarzún, J.; Otero, R.; Torres, T.; Hervé, F. 2010. Estuary deposits in the Río Baguales Formation (Chattian-Aquitanean), Magallanes Province, Chile. Andean Geology 37 (2): 329-344. doi: 10.5027/andgeoV37n2-a04
- Marden, C. 1997. Late-glacial fluctuations of South Patagonian Icefield, Torres del Paine National Park, southern Chile. Quaternary International 38-39: 61-68.
- McCulloch, R.; Bentley, M.; Purves, R.; Hulton, N.; Sugden, D.; Clapperton, C. 2000. Climatic inferences from glacial and palaeoecological evidence at the last glacial termination, southern South America. Journal of Quaternary Science 15 (4): 409-417.
- Mercer, J. 1976. Glacial history of southernmost South America. Quaternary Research 6 (2): 125-166.
- Merriam, D.; Jewett, D. 1989. Methods of thematic map comparison. *In* Current Trends in Geomathics, Plenun press: 9-18. New York.
- Mindrescu, M.; Evans, I.; Cox, N. 2010. Climatic implications of cirque distribution in the Romanian Carpathians: palaeowind directions during glacial periods. Journal of Quaternary Science 25 (6): 875-888.
- Montgomery, D.; Balco, G.; Willett, S. 2001. Climate, tectonics, and the morphology of the Andes. Geology 29 (7): 579-582.
- Moreno, P.; Francois, J.; Moy, C.; Villa-Martínez, R. 2010. Covariability of the Southern Westerlies and atmospheric CO, during the Holocene. Geology 38 (8): 727-730.
- Moreno, P.; Francois, J.; Villa-Martínez, R.; Moy, C. 2009.
 Millennial-scale variability in Southern Hemisphere
 Westerly Wind activity over the last 5000 years in SW
 Patagonia. Quaternary Science Reviews 28: 25-38.
- Olyphant, G. 1981. Allometry and cirque evolution. Geological Society of America Bulletin 92 (9): 679-685.
- Peña, H.; Gutiérrez, R. 1992. Statistical analysis of precipitation and air temperature in the Southern Patagonian Icefield. *In Glaciological Researches in Patagonia*, Nagoya, Japanese Society of Snow and Ice, Data Center for Glacier Research: 95-108.
- Rabassa, J.; Coronato, A. 2009. Glaciations in Patagonia and Tierra del Fuego during the Ensenadan Stage/

- Age (Early Pleistocene-earliest Middle Pleistocene). Quaternary International 210 (1-2): 18-36.
- Rabassa, J.; Coronato, A.; Salemme, M. 2005. Chronology of the Late Cenozoic Patagonian glaciations and their correlation with biostratigraphic units of the Pampean region (Argentina). Journal of South American Earth Sciences 20 (1-2): 81-103.
- Rabassa, J.; Coronato, A.; Martínez, O. 2011. Late Cenozoic glaciations in Patagonia and Tierra del Fuego: an updated review. Biological Journal of the Linnean Society 103 (25): 316-335.
- Ramos, V. 1989. Andean foothills structures in northern Magallanes Basin, Argentina. AAPG Bulletin 73 (7): 887-903. doi: 10.1306/44B4A28A-170A-11D7-8645000102C1865D.
- Ramos, V.; Ghiglione, M. 2008. Tectonic evolution of the Patagonian Andes. *In* The Late Cenozoic of Patagonia and Tierra del Fuego. Elsevier: 57-71. Amsterdam.
- Rodbell, D.; Smith, J.; Mark, B. 2009. Glaciation in the Andes during the Late Glacial and Holocene. Quaternary Science Reviews 28 (21-22): 2165-2212.
- Ruiz-Fernández, J.; Poblete-Piedrabuena, M.; Serrano-Muela, M.; Martí-Bono, C.; García-Ruiz, J. 2009. Morphometry of glacial cirques in the Cantabrian Range (Northwest Spain). Zeitschriftfür Geomorphologie 53 (1): 47-68.
- Sagredo, E.; Moreno, P.; Villa-Martínez, R.; Kaplan, M.; Kubik, P.; Stern, C. 2011. Fluctuations of the Última Esperanza ice lobe (52°S), Chilean Patagonia, during the last glacial maximum and termination 1. Geomorphology 125: 92-108.
- Sepúlveda, S.; Le Roux, J.P.; Palma, G. 2013. Application of the composite maps method for landslide susceptibility assessment and its potential use for other natural risk analyses. Investigaciones Geográficas 46: 47-56.
- Solari, M.A.; Calderón, M.; Airo, A.; Le Roux, J.P.; Hervé, F. 2012. Evolution of the Great Tehuelche Paleolake in the Torres del Paine National Park of Chilean Patagonia during the Last Glacial Maximum and Holocene. Andean Geology 39 (1): 1-21. doi: 10.2225/vol14-issue3-fulltext-10.
- Steffanova, P.; Mentlík, P. 2007. Comparison of morphometric characteristics of cirques in the Bohemian Forest. Silva Gabreta 13 (3): 191-204.
- Strelin, J.; Malagnino, E. 2000. Late-glacial history of Lago Argentino, Argentina, and age of the Puerto Bandera moraines. Quaternary Research 54 (3): 339-347.
- Strelin, J.; Denton, G.; Vandergoes, M.; Ninnemman, U.; Putman, A. 2011.Radiocarbon chronology of the late-glacial Puerto Bandera moraines, Southern Patagonian Icefield, Argentina. Quaternary Science Reviews 30: 2551-2569.

- Strelin, J.; Kaplan, M.; Vandergoes, M.; Denton, G.; Schaefer, J. 2014. Holocene glacier history of the Lago Argentino basin, Southern Patagonian Icefield. Quaternary Science Reviews 101: 124-145.
- Sudgen, D.; Bentley, M.; Fogwill, C.; Hulton, N.; McCulloch, R.; Purves, R. 2005. Late-glacial glacier events in southernmost south America: A blend of
- "northern" and "southern" hemispheric climatic signals? Geografiska Annaler, Series A: Physical Geography 87 (2): 273-288.
- Villa-Martínez, R.; Moreno, P. 2007. Pollen evidence for variations in the southern margin of the Westerly Winds in SW Patagonia over the last 12,600 years. Quaternary Research 68: 400-409.

Manuscript received: July 19, 2016; revised/accepted: January 25, 2018; available online: May 31, 2018.